Cell Reports
Physical Science

CellPress
OPEN ACCESS

Article

Infrared spectroscopic signature of the structural diversity of the water heptamer

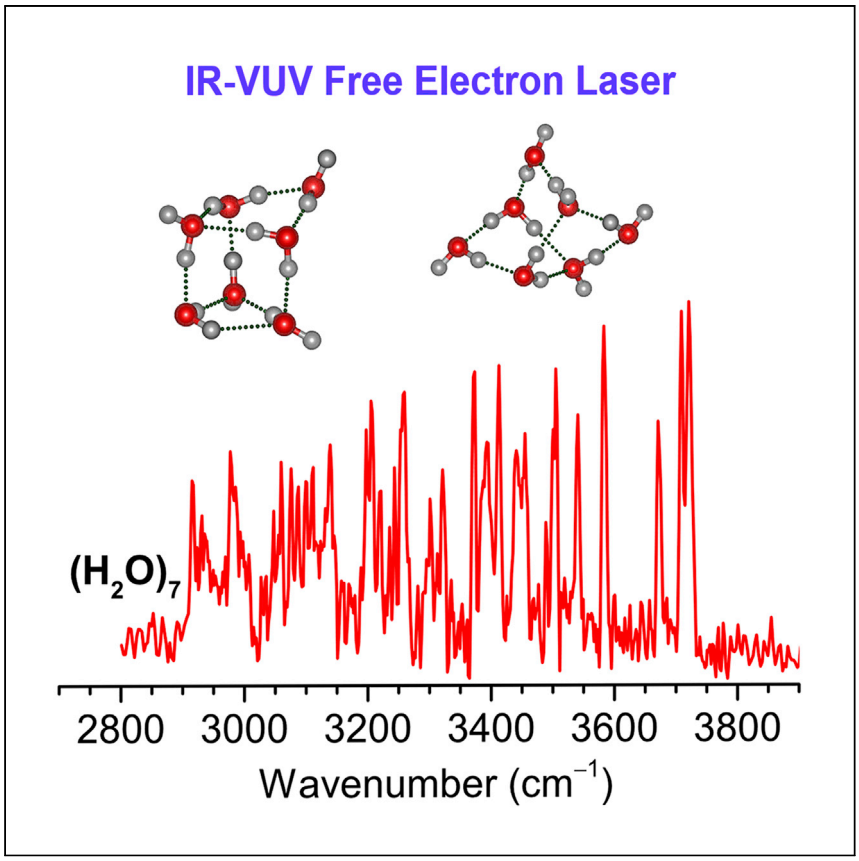

Spectroscopic and quantum investigation of $(H_2O)_7$ is critical in understanding the hydrogen-bonding network transitions between liquid water and ice. Zhang et al. report the infrared spectra of neutral $(H_2O)_7$ based on threshold photoionization using a tunable vacuum ultraviolet free electron laser and computational modeling. Two classes of prism- and cage-like structures are identified.

Yang-Yang Zhang, Chong Wang, Gang Li, ..., Ling Jiang, Xueming Yang, Jun Li

ljiang@dicp.ac.cn (L.J.)
xmyang@dicp.ac.cn (X.Y.)
junli@mail.tsinghua.edu.cn (J.L.)

Highlights

Size-specific infrared spectra of neutral water heptamer $(H_2O)_7$ is reported

Many nearly isoenergetic isomers are found to present at finite temperatures

Two classes of prism- and cage-like structures are identified

Zhang et al., Cell Reports Physical Science 3, 100748
February 16, 2022
https://doi.org/10.1016/j.xcrp.2022.100748

Cell Reports
Physical Science

CellPress
OPEN ACCESS

Article

Infrared spectroscopic signature of the structural diversity of the water heptamer

Yang-Yang Zhang,[1,5] Chong Wang,[2,3,5] Gang Li,[2,5] Xiangyu Zang,[2] Yong Yu,[2] Han-Shi Hu,[1] Jiayue Yang,[2] Weiqing Zhang,[2] Dongxu Dai,[2] Guorong Wu,[2] Ling Jiang,[2,6,*] Xueming Yang,[2,4,*] and Jun Li[1,4,*]

SUMMARY

As a key species in understanding the hydrogen-bonding network transitions between liquid water and ice, the neutral water heptamer is a challenging experimental target, owing to the richness of low-lying isomers. Here, we report the size-specific infrared spectra of confinement-free, neutral water heptamer $(H_2O)_7$ based on threshold photoionization using a tunable vacuum ultraviolet free electron laser. The complexity of the observed spectra indicates that many nearly isoenergetic isomers are present at finite temperatures. Two classes of prism- and cage-like structures are identified in a high-pressure pulsed supersonic expansion of water heptamer, in which the former is favored energetically at low temperatures and serves as a major contributor to the experimental spectrum. These findings provide key information for filling the gap between well-studied water hexamer and octamer.

INTRODUCTION

Water clusters have become a superb benchmark for accurate description of the hydrogen-bonding interactions that operate in liquid water and ice.[1–6] Extensive efforts have been devoted to the spectroscopic characterization of charged water clusters, such as $(H_2O)_n^+$, $(H_2O)_n^-$, and $H^+(H_2O)_n$, for which size selection and detection are straightforward. Along with significant advances in quantum theoretical calculations, these studies provided essential insights into the structures and dynamics of ionic water clusters. For instance, the hydrogen bond (HB) networks of protonated water clusters, $H^+(H_2O)_n$ were found to evolve from the chain structures ($n \leq 10$) into two-dimensional (2D) net structures ($\sim 10 < n < 21$), and then into nanometer-scaled cages ($n \geq 21$).[7,8]

The HB network structures in neutral water clusters $(H_2O)_n$ are substantially different from those in ionic ones. Previous experimental and theoretical work revealed that the water trimer, tetramer, and pentamer all have cyclic global-minimum structures with all oxygen atoms in a 2D plane; the water hexamer is the smallest water cluster with a 3D HB network of prism; the water octamer is the smallest water cluster with pseudo-cubic structures.[9–22] Very recently, we set up an infrared spectroscopic facility based on threshold photoionization using a tunable vacuum ultraviolet free electron laser (VUV-FEL),[23,24] which allows for size selection of neutral clusters. With this new technique, the access to transient low-lying structures of water clusters becomes possible. We find at finite temperatures a higher-energy noncyclic isomer of water pentamer represents the 2D to 3D transition of water cluster.[25] For the water octamer, two chiral isomers with C_2 symmetry and one isomer with C_i symmetry are also identified.[26]

[1]Key Laboratory of Organic Optoelectronics & Molecular Engineering of the Ministry of Education, Department of Chemistry, Tsinghua University, Beijing 100084, China

[2]State Key Laboratory of Molecular Reaction Dynamics, Dalian Institute of Chemical Physics, Chinese Academy of Sciences, Dalian 116023, China

[3]University of Chinese Academy of Sciences, 19A Yuquan Road, Beijing 100049, China

[4]Department of Chemistry, Southern University of Science and Technology, Shenzhen 518055, China

[5]These authors contributed equally

[6]Lead contact

*Correspondence: ljiang@dicp.ac.cn (L.J.), xmyang@dicp.ac.cn (X.Y.), junli@mail.tsinghua.edu.cn (J.L.)

https://doi.org/10.1016/j.xcrp.2022.100748

The water heptamer, $(H_2O)_7$, is of considerable interest in the context of so-called amorphous precursor to the "crystal-like" cubic structures.[16,17] Inasmuch as the water hexamer and octamer possess "3 + 3" prism and "4 + 4" cube structures of water cluster pairs, respectively, the isomers of water heptamer are particularly rich because the competition of the two structural motifs. Previous quantum chemical calculations predicted many structural landscapes of low-lying isomers for $(H_2O)_7$,[22,27–31] which can be classified into six conformer classes based on their hydrogen-bonding topology, including the Prism (PR), Cage (CA), Book, Tetrahedral Water (TW), Cyclic Hexamer + Monomer (CY), and Ring motifs. Free energy calculations showed that the PR structures maintain the Gibbs free energy minimum until approximately 200 K, at which point the Book structures become favored energetically because of entropic effects.[31,32] Experimentally, helium-scattering infrared (IR) spectroscopy in a continuous supersonic expansion identified two lowest-energy PR isomers.[33] Recent broadband Fourier transform rotational spectroscopy indicated that the global-minimum PR isomer is the dominant water heptamer species present in the experimental condition of a pulsed supersonic expansion, and that either a higher-energy PR or CA isomer contributes in a minor way to the experimental spectrum.[34] While a PR structure derived from the D_{2d}-symmetry cubic water octamer was tentatively assigned in the IR-ultraviolet (IR-UV) double resonance spectrum of phonel-$(H_2O)_7$,[35] a S_4-derived PR isomer was captured in an IR-UV experiment on benzene-$(H_2O)_7$.[36] Although several structures of $(H_2O)_7$ are identified, the rich hydrogen-bonding networks of numerous low-lying isomers for $(H_2O)_7$ have eluded direct spectral observation. Here, we report the size-specific IR spectroscopic signature of a confinement-free, neutral water heptamer based on threshold photoionization using a tunable VUV-FEL and computational modeling of the structures and spectra. The agreement between theory and experiment provides evidence of co-existence of both PR and CA motifs in a high-pressure pulsed supersonic expansion condition.

RESULTS AND DISCUSSION

Experimental results

The experimental IR spectrum of $(H_2O)_7$ is shown in Figure 1A and the band positions are listed in Table 1. The IR spectrum of the water heptamer consists of at least 30 vibrational bands. In contrast, the IR spectrum of the "crystal-like" cubic octamer $(H_2O)_8$ exhibits three groups of well-separated and distinct bands that correspond to single H-donor OH, double H-donor OH, and H-donor-free OH stretching modes.[16–18] The complex IR spectrum of $(H_2O)_7$ suggests possible contributions from a broad range of so-called amorphous hydrogen-bonding configurations at finite temperatures. As shown in Figure S1, the present spectrum with improved resolution displays several new absorptions at 2,915 (labeled S_1), 3,205 (S_5), 3,373 (S_8), 3,393 (D_1), 3,505 (D_4), and 3,709 cm^{-1} (F_1) when compared with the previous spectra. The 3,259 cm^{-1} (S_6) band that had low intensity in the helium-scattering IR spectrum[33] is now observed with high intensity.

Geometries and relative stabilities

Our global-minimum structural search (*infra vide*) found 516 independent structures for $(H_2O)_7$, which indicate more low-energy isomers than reported previously.[22,27–36] The nomenclature (PR, CA, Book, TW, CY, and Ring) for the structures of $(H_2O)_7$ follows the literature.[22,27–36] The selected lowest-energy structures for each conformer group are shown in Figure 2. The structures lying within 6 kcal/mol are illustrated in Figures S2–S4 for comparison.

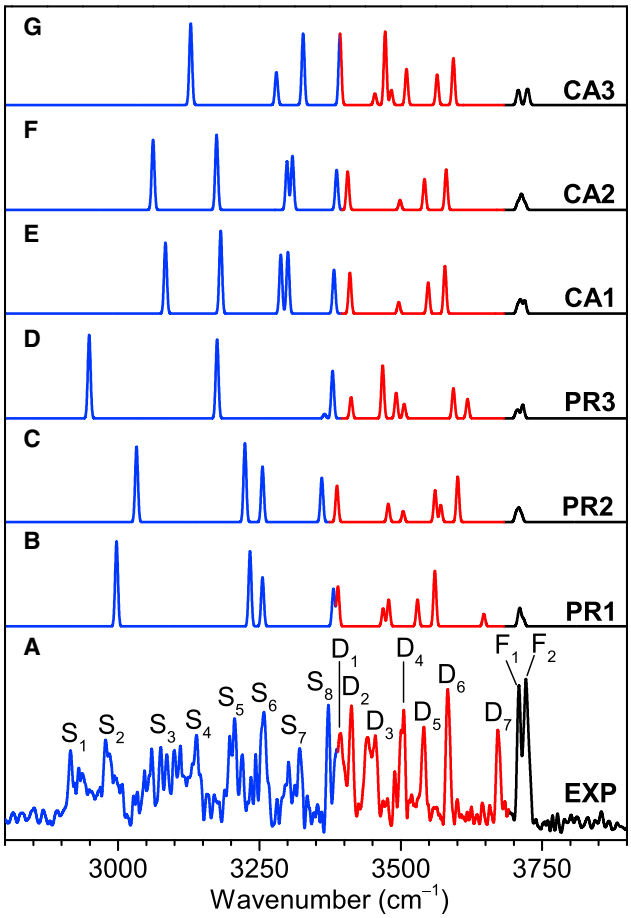

Figure 1. Comparison of experimental and simulated IR spectra of the water heptamer

(A) Experimental IR spectrum of $(H_2O)_7$, where the OH stretch fundamentals assigned to single H-donor OH stretch (S, blue), double H-donor OH stretch (D, red), and H-donor-free OH (F, black) are indicated.

(B–G) Simulated IR spectra of the three lowest-energy isomers with the prism- and cage-like geometries (PR*n* and CA*n*, *n* = 1–3), where the calculations were performed at the MP2/AVDZ level, with the harmonic frequencies scaled by 0.956.

The lowest-energy isomer of $(H_2O)_7$ is verified to be PR1, which can be derived from the hexamer prism by inserting the seventh water molecule as single-donor single-acceptor to one of the triangles. Our MP2/AVDZ calculation shows that the PR2 and PR3 isomers lie only 0.51 and 0.84 kcal/mol above the lowest-energy PR1 isomer (Figure 2), respectively. At the same theoretical level, the CA, Book, TW, CY, and Ring structures are located higher in energy than the global-minimum PR1 isomer by 1.22, 2.57, 2.78, 4.45, and 5.04 kcal/mol (Figure 2), respectively. These calculated results are consistent with the previous studies.[22,27–36]

The Gibbs free energies of the PR1, CA1, Book1, TW1, CY1, and Ring1 isomers were calculated at the MP2/AVDZ level for the vibrational analyses. The relative free energies ΔG at 1 atm pressure in the range of T = 0–400 K for the CA1, Book1, TW1, CY1, and Ring1 isomers are plotted in Figure 3, with the free energy of the PR1 isomer as reference. Due to the structural diversity, the vibrational entropies of the water heptamer isomers behave differently upon temperature increase. While the free energy difference $\Delta G_{CA1\text{-}PR1}$ slightly decreases when temperature increases, the $\Delta G_{Book1\text{-}PR1}$, $\Delta G_{TW1\text{-}PR1}$,

Table 1. Experimental vibrational frequencies and band assignments for $(H_2O)_7$

Label	Frequency (cm^{-1})	Assignment
S_1	2,915	single H-donor OH stretch
S_2	2,983	
S_3	3,033–3,111	
S_4	3,139	
S_5	3,205	
S_6	3,259	
S_7	3,321	
S_8	3,373	
D_1	3,393	double H-donor OH stretch
D_2	3,413	
D_3	3,455	
D_4	3,505	
D_5	3,541	
D_6	3,583	
D_7	3,671	
F_1	3,709	H-donor-free OH
F_2	3,721	

$\Delta G_{CY1\text{-}PR1}$, and $\Delta G_{Ring1\text{-}PR1}$ exhibit remarkable temperature dependence. This observation is due to the fact that the Book, TW, CY, and Ring structures are less constrained by HBs and become entropically favorable at higher temperatures, while the PR and CA structures are more similar. Below 200 K, the PR and CA isomers are more stable than other isomers. At 270 K, the TW1 isomer becomes the most stable structure. At 350 K, the Ring1 isomer becomes the most stable structure.

As shown previously, the HB interaction between a proton donor and an adjacent oxygen lone-pair acceptor is mainly responsible for the stability of water clusters.[25,37] The HB number of the PR1, CA1, Book1, TW1, CY1, and Ring1 isomers is 10, 9, 8, 8, 8, and 7 (Table 2), respectively. Our EDA-NOCV theoretical analysis shows that the contribution of HB energy to the total orbital interaction energy ($\Delta E_{HB}/\Delta E_{total}$) for isomers PR1, CA1, Book1, TW1, CY1, and Ring1 is 89.2%, 88.5%, 87.9%, 88.7%, 87.8%, and 86.9% (Table 2), respectively. These results support the relative stabilities of these six conformer groups.

Comparison of experimental and calculated IR spectra

As global-minimum structures of water hexamer and octamer featuring high-symmetry "3 + 3" and "4 + 4" assembling of water cluster pairs have rather high stability (Figure S5),[11,15–22] the heptamer isomers suffer from the competition of "6 + 1" and "8 − 1" structural motifs. As a result, there exists a wide variety of low-lying isomers for the water heptamer, which makes it cumbersome to unambiguously assign all the vibrational bands for the water heptamer. Considering that these clusters were generated by means of a high-pressure pulsed valve that is capable of producing very cold molecular beam conditions[38] and that the temperature of the water heptamer could be far below 200 K, low-lying isomers could be trapped by rapid cooling under this supersonic jet expansion.[39] On the basis of the preferred stabilities of PR and CA structures below 200 K, a qualitative assignment of the spectra is aided by the comparison of experimental and calculated IR spectra of the selected PR and CA isomers (Figure 1).

It can be seen from Figure 2 that there are three general classes of hydrogen-bonding sites of $(H_2O)_7$, which we classify as AD, ADD, and AAD configurations

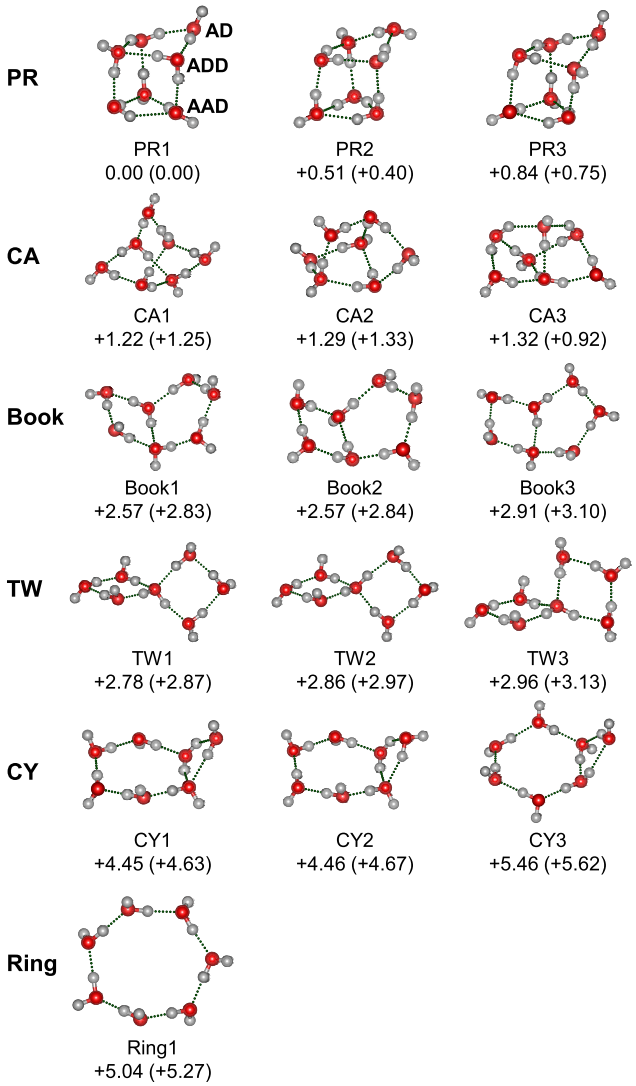

Figure 2. Low-lying structures of the water heptamer

The isomers are denoted by PR (Prism), CA (Cage), Book, TW (Tetrahedral Water), CY (Cyclic Hexamer + Monomer), and Ring. Relative energies from MP2/AVDZ and DLPNO-CCSD(T)/AVTZ (in parentheses) are listed in kcal/mol. The structures consist of three general classes of hydrogen-bonding sites that we classify as AD, ADD, and AAD configurations according to the number of acceptor (A) and donor (D) hydrogen bonds, respectively.

according to the number of acceptor (A) and donor (D) HBs, respectively. Accordingly, each isomer possesses three types of OH groups: single H-donor OH, double H-donor OH, and H-donor-free OH groups. As noted previously,[16–18] the AAD → ADD HBs are remarkably shorter than ADD → AAD HBs, and the corresponding frequency of single H-donor OH stretch is lower than that of double H-donor OH stretch. As a result, the vibrational bands of single H-donor OH (labeled S), double H-donor OH (labeled D), and H-donor-free (labeled F) OH groups are well spread out in the IR spectra (Figure 1).

In the calculated spectrum of isomer PR1 (Figure 1B), the lowest frequency vibration (2,997 cm^{-1}) arises from the single H-donor OH stretch and agrees with the experimental band S_2 (2,983 cm^{-1}). The calculated bands at 3,233 and 3,255 cm^{-1} attributed

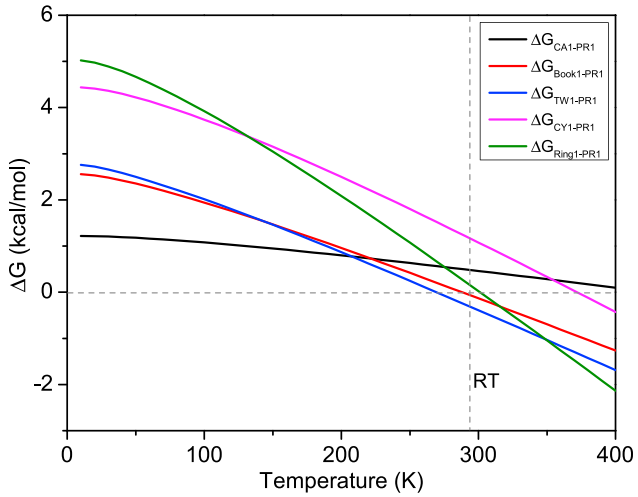

Figure 3. Free energies of isomers CA1, BooK1, TW1, CY1, and Ring1 relative to isomer PR1 as a function of temperature

RT, room temperature (298.15 K). Calculations were carried out at the MP2/AVDZ level.

to the single H-donor OH stretches are consistent with the experimental bands S_5 (3,205 cm^{-1}) and S_6 (3,259 cm^{-1}), respectively. The calculated double H-donor OH stretches (3,389, 3,479, 3,530, 3,560, and 3,647 cm^{-1}) account for the experimental bands D_1, D_4, D_5, D_6, and D_7 (3,393, 3,505, 3,541, 3,583, and 3,671 cm^{-1}), respectively. The calculated spectrum of isomer PR1 alone is much too simple to explain the experimental spectrum. The calculated IR spectra of isomers PR2, PR3, CA1, CA2, and CA3 agree well with the experimental spectrum and help to account for the remaining unassigned bands at finite temperature. Note that the calculated vibrational spectra below 3,300 cm^{-1} could be shifted due to the Fermi resonance interactions between the water bend overtone and the stretching modes,[40–43] and given the number of similar bonding motifs that are present in similar Prism, Cage, etc., structures, the assignment of all of the vibrational bands for $(H_2O)_7$ is cumbersome.

As shown in Figure S5, in the cyclic structures of $(H_2O)_n$ (n = 3–5), each water molecule accepts a single HB and donates another HB, which corresponds to an AD site with its H-donor-free OH stretch appearing in the range 3,720–3,729 cm^{-1}. When the water molecule acts as an acceptor for a third HB, an AAD site is formed with the indication of a lower OH frequency as compared with the AD site.[7,44] In this context, the well-separated free OH bands F_1 (3,709 cm^{-1}) and F_2 (3,721 cm^{-1}) observed in the IR spectrum of $(H_2O)_7$ correspond to two distinct AD and AAD sites. For the PR1 isomer, the calculated H-donor-free OH stretches exhibit a broad feature (Figure 1B), in which the free OH groups of AAD water appear at 3,710 cm^{-1} and those of AD water appear at 3,717 cm^{-1}. The band position of calculated H-donor-free OH stretches can be tentatively assigned to the experimental bands F_1 (3,709 cm^{-1}), although the calculated separation gap of the free OH stretches at AAD and AD sites (7 cm^{-1}) is smaller than the experimental value (12 cm^{-1}). The experimental bands F_1 and F_2 appear to match the H-donor-free OH stretches of the CA3 isomer (Figure 1G). The contribution for the experimental spectrum can be mainly from the energetically favorable PR structures, although the minor contribution of CA structures cannot be ruled out.

In summary, the OH vibrational stretch spectra are reported for neutral $(H_2O)_7$ using VUV-FEL-based IR spectroscopy. Electronic structure calculations using the

Table 2. The analysis of the hydrogen-bonding interaction of $(H_2O)_7$

Isomer	Number of HBs	$\Delta E_{HB}/\Delta E_{total}$ (%)	ΔE_{total} (kcal/mol)
PR1	10	89.2	0.00
CA1	9	88.5	1.22
Book1	8	87.9	2.57
TW1	8	88.7	2.78
CY1	8	87.8	4.45
Ring1	7	86.9	5.04

The number of hydrogen bonds (HBs) and the percentage of the contribution of HB energy to the total orbital interaction energy ($\Delta E_{HB}/\Delta E_{total}$) of the representative low-energy isomers for $(H_2O)_7$. ΔE_{total} corresponds to the MP2/AVDZ relative energies.

constrained basin-hopping global-minimum structural search and *ab initio* MP2 methods have been performed to determine the structures of the low-lying isomers. A variety of diverse bands observed in the IR spectrum of the water heptamer provide evidence for the presence of various low-lying structures at finite temperatures. The consistency of the experimental and calculated infrared spectra allow us to establish general trends in the structural motifs. We find that the major contribution for the experimental spectrum originates from the prism-like isomers, although the minor contribution of the higher-energy cage-like isomers is non-negligible. These findings contribute to an improved understanding of structural diversity and complexity of water heptamer in the context of the formation and growth of ordered structures in larger systems. The present data provide new benchmark measurements for the development of highly accurate electronic and vibrational description of HB interactions that can be used for predicting macroscopic properties of bulk water and biological systems.

EXPERIMENTAL PROCEDURES

Resource availability

Lead contact

Further information and requests for resources and reagents should be directed to and will be fulfilled by the lead contact, Ling Jiang (ljiang@dicp.ac.cn).

Materials availability

This study did not generate new unique materials.

Data and code availability

All data needed to evaluate the conclusions in this paper are present in the paper and/or the supplemental information.

Experimental method

Experiments were performed using an infrared-vacuum ultraviolet (IR-VUV) spectroscopy apparatus described previously.[23] Neutral water clusters were generated by supersonic expansions of a water-helium mixture using a high-pressure pulsed valve (Even-Lavie valve, EL-7-2011-HT-HRR) that is capable of producing a very cold molecular beam.[38] The stagnation pressure was approximately 50 bar. The molecular beam passed through a 4-mm diameter skimmer (Beam Dynamics, Model 50.8) and an aperture with a 3-mm opening. The extraction plates of reflectron time-of-flight mass spectrometer (TOF-MS) were powered by a high-voltage direct current (DC) of 2950 V. Charged clusters were deflected out of the molecular beam by the DC electric field of the extraction plates. Neutral water clusters in the beam were threshold ionized by the VUV-FEL pulse and mass-analyzed in a

reflectron TOF-MS. Here, the tunable IR light pulse was introduced at about 30 ns prior to the VUV-FEL pulse in a crossed manner. When the resonant vibrational transition is evoked by the IR laser light and causes vibrational predissociation, a depletion of the selected neutral cluster mass signal can be detected. At 113.10 nm, the IR spectrum of size-selected neutral water heptamer was obtained as a depletion spectrum of the ion signal intensity of $(H_2O)_7^+$ as a function of IR wavelength. The VUV-FEL in the present experiment was operated at 20 Hz and the IR laser was operated at 10 Hz. IR spectra were recorded in the difference mode of operation (IR laser on-IR laser off).

The tunable VUV-FEL light was generated by the Dalian Coherent Light Source (DCLS) facility. With proper optimization of the linear accelerator, a high-quality beam with the emittance down to ~1.5 mm milli-radians, a projected energy spread of ~1%, and a pulse duration of ~1.5 ps can be obtained. For recording the pulse spectral characteristic, an online VUV spectrometer was presented to monitor each single VUV-FEL pulse. The tunable IR laser beam was generated by a potassium titanyl phosphate (KTP)/potassium titanyl arsenate optical parametric oscillator (OPO)/amplifier system (LaserVision) pumped by an injection-seeded Nd:YAG laser (Continuum Surelite EX). This system is tunable from 700 to 7,000 cm^{-1} with a line width of 1 cm^{-1}. The wavelength of the OPO laser output was calibrated using a commercial wavelength meter (HighFinesse GmbH, WS6-200 VIS IR).

Computational methods

Global-minimum structural search based on density functional theory was carried out for $(H_2O)_7$ using TGMin code.[45–47] Quantum chemical calculations were carried out to refine the energies of the low-lying isomers (within 6 kcal/mol) at the *ab initio* MP2/aug-cc-pVDZ (abbreviated as AVDZ throughout) level using the Gaussian 09 package.[48] Harmonic vibrational frequencies were calculated with analytical second derivatives of the total energy. A scaled factor of 0.956 was used for harmonic vibrational frequencies to account for the systematic errors in the calculations.[49] The MP2/AVDZ relative energies were calculated at 0 K with corrections of zero-point vibrational energies. The *ab initio* DLPNO-CCSD(T)/aug-cc-pVTZ (AVTZ) relative energies were calculated on the MP2/AVDZ optimized geometries with the ORCA program,[50–52] which included the MP2/AVDZ zero-point vibrational energy corrections. Gibbs free energies G(T) = U(T) + PV – TS were calculated with statistical mechanics, where U, S, P, V, and T stand for the internal energy, entropy, pressure, volume, and temperature, respectively.

The nature of the hydrogen-bonding interaction in $(H_2O)_7$ was analyzed with the EDA-NOCV analyses (energy decomposition analysis-natural orbitals for chemical valence)[53] at the level of GGA PBE/TZ2P[54] using the Amsterdam Density Functional program (ADF 2016.101).[55] The EDA-NOCV scheme provides both qualitative ($\Delta\rho_{orb}$) and quantitative (ΔE_{orb}) information about the strength and contribution of orbital interactions in chemical bonding, as demonstrated in the study of water clusters $(H_2O)_n$ (n = 2–6 and 8).[25,26] We used the unrelaxed water fragments from the optimized structures to derive the intrinsic binding energies of water clusters.

SUPPLEMENTAL INFORMATION

Supplemental information can be found online at https://doi.org/10.1016/j.xcrp.2022.100748.

ACKNOWLEDGMENTS

The authors gratefully acknowledge the DCLS for VUV-FEL beam time and the DCLS staff for support and assistance. This work was supported by the National Natural Science Foundation of China (92061203, 21688102, and 22033005), the Strategic Priority Research Program of Chinese Academy of Sciences (CAS) (XDB17000000), the International Partnership Program of CAS (121421KYSB20170012), the Dalian Institute of Chemical Physics (DICP DCLS201702), CAS (GJJSTD20190002), the Science Challenge Project (TZ2016004), and the Guangdong Provincial Key Laboratory of Catalysis (no. 2020B121201002). The calculations were performed with SUSTech supercomputer.

AUTHOR CONTRIBUTIONS

Y.-Y.Z., H.-S.H., and J.L. conducted the theoretical calculations and data analysis. C.W., G.L., X.Z., Y.Y., J.Y., W.Z., D.D., G.W., L.J., and X.Y. conducted the experiments and data analysis. L.J., X.Y., and J.L. designed the research and co-wrote the manuscript.

DECLARATION OF INTERESTS

The authors declare no competing interests.

Received: August 10, 2021
Revised: November 29, 2021
Accepted: January 11, 2022
Published: February 1, 2022

REFERENCES

1. Liu, K., Cruzan, J.D., and Saykally, R.J. (1996). Water clusters. Science *271*, 929–933.
2. Buck, U., and Huisken, F. (2000). Infrared spectroscopy of size-selected water and methanol clusters. Chem. Rev. *100*, 3863–3890.
3. Ludwig, R. (2001). Water: from clusters to the bulk. Angew. Chem. Int. Ed. *40*, 1808–1827.
4. Robertson, W.H., and Johnson, M.A. (2003). Molecular aspects of halide ion hydration: the cluster approach. Annu. Rev. Phys. Chem. *54*, 173–213.
5. Young, R.M., and Neumark, D.M. (2012). Dynamics of solvated electrons in clusters. Chem. Rev. *112*, 5553–5577.
6. Samanta, A.K., Wang, Y., Mancini, J.S., Bowman, J.M., and Reisler, H. (2016). Energetics and predissociation dynamics of small water, HCl, and mixed HCl-water clusters. Chem. Rev. *116*, 4913–4936.
7. Miyazaki, M., Fujii, A., Ebata, T., and Mikami, N. (2004). Infrared spectroscopic evidence for protonated water clusters forming nanoscale cages. Science *304*, 1134–1137.
8. Shin, J.W., Hammer, N.I., Diken, E.G., Johnson, M.A., Walters, R.S., Jaeger, T.D., Duncan, M.A., Christie, R.A., and Jordan, K.D. (2004). Infrared signature of structures associated with the $H^+(H_2O)_n$ (n = 6 to 27) clusters. Science *304*, 1137–1140.
9. Vernon, M.F., Lisy, J.M., Krajnovich, D.J., Tramer, A.J., Kwok, H.-S., Shen, Y.R., and Lee, Y.T. (1982). Vibrational predissociation spectra and dynamics of small molecular clusters of H_2O and HF. Faraday Discuss. *73*, 387–397.
10. Pugliano, N., and Saykally, R.J. (1992). Measurement of quantum tunneling between chiral isomers of the cyclic water trimer. Science *257*, 1937–1940.
11. Pribble, R.N., and Zwier, T.S. (1994). Size-specific infrared spectra of benzene-$(H_2O)_n$ clusters (n = 1 through 7): evidence for noncyclic $(H_2O)_n$ structures. Science *265*, 75–79.
12. Cruzan, J.D., Braly, L.B., Liu, K., Brown, M.G., Loeser, J.G., and Saykally, R.J. (1996). Quantifying hydrogen bond cooperativity in water: VRT spectroscopy of the water tetramer. Science *271*, 59–62.
13. Liu, K., Brown, M.G., Cruzan, J.D., and Saykally, R.J. (1996). Vibration-rotation tunneling spectra of the water pentamer: structure and dynamics. Science *271*, 62–64.
14. Liu, K., Liu, K., Brown, M.G., Carter, C., Saykally, R.J., Gregory, J.K., and Clar, D.C. (1996). Characterization of a cage form of the water hexamer. Nature *381*, 501–503.
15. Huisken, F., Kaloudis, M., and Kulcke, A. (1996). Infrared spectroscopy of small size-selected water clusters. J. Chem. Phys. *104*, 17–25.
16. Gruenloh, C.J., Carney, J.R., Arrington, C.A., Zwier, T.S., Fredericks, S.Y., and Jordan, K.D. (1997). Infrared spectrum of a molecular ice cube: the S_4 and D_{2d} water octamers in benzene-$(water)_8$. Science *276*, 1678–1681.
17. Buck, U., Ettischer, I., Melzer, M., Buch, V., and Sadlej, J. (1998). Structure and spectra of three-dimensional $(H_2O)_n$ clusters, n = 8, 9, 10. Phys. Rev. Lett. *80*, 2578–2581.
18. Gruenloh, C.J., Carney, J.R., Hagemeister, F.C., Arrington, C.A., and Zwier, T.S. (1998). Resonant ion-dip infrared spectroscopy of the S_4 and D_{2d} wafer octamers in benzene-$(water)_8$ and benzene$_2$-$(water)_8$. J. Chem. Phys. *109*, 6601–6614.
19. Perez, C., Muckle, M.T., Zaleski, D.P., Seifert, N.A., Temelso, B., Shields, G.C., Kisiel, Z., and Pate, B.H. (2012). Structures of cage, prism, and book isomers of water hexamer from broadband rotational spectroscopy. Science *336*, 897–901.
20. Richardson, J.O., Pérez, C., Lobsiger, S., Reid, A.A., Temelso, B., Shields, G.C., Kisiel, Z., Wales, D.J., Pate, B.H., and Althorpe, S.C. (2016). Concerted hydrogen-bond breaking by quantum tunneling in the water hexamer prism. Science *351*, 1310–1313.
21. Cole, W.T.S., Farrell, J.D., Wales, D.J., and Saykally, R.J. (2016). Structure and torsional dynamics of the water octamer from THz laser spectroscopy near 215 μm. Science *352*, 1194–1197.
22. Rakshit, A., Bandyopadhyay, P., Heindel, J.P., and Xantheas, S.S. (2019). Atlas of putative minima and low-lying energy networks of water clusters n = 3-25. J. Chem. Phys. *151*, 214307.
23. Zhang, B., Yu, Y., Zhang, Z., Zhang, Y.Y., Jiang, S., Li, Q., Yang, S., Hu, H.S., Zhang, W., Dai, D.,

et al. (2020). Infrared spectroscopy of neutral water dimer based on a tunable vacuum ultraviolet free electron laser. J. Phys. Chem. Lett. *11*, 851–855.

24. Li, G., Wang, C., Li, Q., Zheng, H., Wang, T., Yu, Y., Su, M., Yang, D., Shi, L., Yang, J., et al. (2020). Infrared + vacuum ultraviolet two-color ionization spectroscopy of neutral metal complexes based on a tunable vacuum ultraviolet free-electron laser. Rev. Sci. Instrum. *91*, 034103.

25. Zhang, B., Yu, Y., Zhang, Y.Y., Jiang, S., Li, Q., Hu, H.S., Li, G., Zhao, Z., Wang, C., Xie, H., et al. (2020). Infrared spectroscopy of neutral water clusters at finite temperature: evidence for a noncyclic pentamer. Proc. Natl. Acad. Sci. U S A. *117*, 15423–15428.

26. Li, G., Zhang, Y.Y., Li, Q., Wang, C., Yu, Y., Zhang, B., Hu, H.S., Zhang, W., Dai, D., Wu, G., et al. (2020). Infrared spectroscopic study of hydrogen bonding topologies in the smallest ice cube. Nat. Commun. *11*, 5449.

27. Jensen, J.O., Krishnan, P.N., and Burke, L.A. (1995). Theoretical study of water clusters: Heptamers. Chem. Phys. Lett. *241*, 253–260.

28. Kryachko, E.S. (1997). Norbornane-type water heptamer. Chem. Phys. Lett. *272*, 132–138.

29. Kim, J., Majumdar, D., Lee, H.M., and Kim, K.S. (1999). Structures and energetics of the water heptamer: comparison with the water hexamer and octamer. J. Chem. Phys. *110*, 9128–9134.

30. Sadlej, J., Buch, V., Kazimirski, J.K., and Buck, U. (1999). Theoretical study of structure and spectra of cage clusters $(H_2O)_n$, n = 7-10. J. Phys. Chem. A. *103*, 4933–4947.

31. Shields, R.M., Temelso, B., Archer, K.A., Morrell, T.E., and Shields, G.C. (2010). Accurate predictions of water cluster formation, $(H_2O)_n$ (n = 2-10). J. Phys. Chem. A. *114*, 11725–11737.

32. Temelso, B., Archer, K.A., and Shields, G.C. (2011). Benchmark structures and binding energies of small water clusters with anharmonicity corrections. J. Phys. Chem. A. *115*, 12034–12046.

33. Brudermann, J., Melzer, M., and Buck, U. (1999). The asymmetric cage structure of $(H_2O)_7$ from a combined spectroscopic and computational study. J. Chem. Phys. *110*, 10649–10652.

34. Perez, C., Lobsiger, S., Seifert, N.A., Zaleski, D.P., Temelso, B., Shields, G.C., Kisiel, Z., and Patea, B.H. (2013). Broadband Fourier transform rotational spectroscopy for structure determination: the water heptamer. Chem. Phys. Lett. *571*, 1–15.

35. Janzen, C., Spangenberg, D., Roth, W., and Kleinermanns, K. (1999). Structure and vibrations of phenol$(H_2O)_{7,8}$ studied by infrared-ultraviolet and ultraviolet-ultraviolet double-resonance spectroscopy and ab initio theory. J. Chem. Phys. *110*, 9898–9907.

36. Tabor, D.P., Kusaka, R., Walsh, P.S., Sibert, E.L., III, and Zwier, T.S. (2015). Isomer-specific spectroscopy of benzene-$(H_2O)_n$, n = 6,7: benzene's role in reshaping water's three-dimensional networks. J. Phys. Chem. Lett. *6*, 1989–1995.

37. Reed, A.E., and Weinhold, F. (1983). Natural bond orbital analysis of near-Hartree-Fock water dimer. J. Chem. Phys. *78*, 4066–4073.

38. Even, U., Jortner, J., Noy, D., Lavie, N., and Cossart-Magos, C. (2000). Cooling of large molecules below 1 K and He clusters formation. J. Chem. Phys. *112*, 8068–8071.

39. Jordan, K.D. (2019). Smallest water clusters supporting the ice I structure. Proc. Natl. Acad. Sci. U S A. *116*, 24383–24385.

40. Wang, Y., and Bowman, J.M. (2013). IR spectra of the water hexamer: theory, with inclusion of the monomer bend overtone, and experiment are in agreement. J. Phys. Chem. Lett. *4*, 1104–1108.

41. Howard, J.C., and Tschumper, G.S. (2015). Benchmark structures and harmonic vibrational frequencies near the CCSD(T) complete basis set limit for small water clusters: $(H_2O)_{n = 2, 3, 4, 5, 6}$. J. Chem. Theor. Comput. *11*, 2126–2136.

42. Brown, S.E., Götz, A.W., Cheng, X., Steele, R.P., Mandelshtam, V.A., and Paesani, F. (2017). Monitoring water clusters "melt" through vibrational spectroscopy. J. Am. Chem. Soc. *139*, 7082–7088.

43. Kananenka, A.A., and Skinner, J.L. (2018). Fermi resonance in OH-stretch vibrational spectroscopy of liquid water and the water hexamer. J. Chem. Phys. *148*, 244107.

44. Yang, N., Duong, C.H., Kelleher, P.J., McCoy, A.B., and Johnson, M.A. (2019). Deconstructing water's diffuse OH stretching vibrational spectrum with cold clusters. Science *364*, 275–278.

45. Zhao, Y., Chen, X., and Li, J. (2017). TGMin: a global-minimum structure search program based on a constrained basin-hopping algorithm. Nano Res. *10*, 3407–3420.

46. Chen, X., Zhao, Y.-F., Wang, L.-S., and Li, J. (2017). Recent progresses of global minimum searches of nanoclusters with a constrained Basin-Hopping algorithm in the TGMin program. Comput. Theor. Chem. *1107*, 57–65.

47. Chen, X., Zhao, Y.-F., Zhang, Y.-Y., and Li, J. (2019). TGMin: an efficient global minimum searching program for free and surface-supported clusters. J. Comput. Chem. *40*, 1105–1112.

48. Frisch, M.J., Trucks, G.W., Schlegel, H.B., Scuseria, G.E., Robb, M.A., Cheeseman, J.R., Scalmani, G., Barone, V., Mennucci, B., Petersson, G.A., et al. (2013). Gaussian 13, Revision D.01 (Gaussian, Inc.).

49. Alecu, I.M., Zheng, J., Zhao, Y., and Truhlar, D.G. (2010). Computational thermochemistry: scale factor databases and scale factors for vibrational frequencies obtained from electronic model chemistries. J. Chem. Theor. Comput. *6*, 2872–2887.

50. Kendall, R.A., Dunning, T.H., and Harrison, R.J. (1992). Electron-affinities of the 1st-row atoms revisited-systematic basis-sets and wave-functions. J. Chem. Phys. *96*, 6796–6806.

51. Weigend, F., Kohn, A., and Hattig, C. (2002). Efficient use of the correlation consistent basis sets in resolution of the identity MP2 calculations. J. Chem. Phys. *116*, 3175–3183.

52. Neese, F. (2012). The ORCA program system. Wires. Comput. Mol. Sci. *2*, 73–78.

53. Mitoraj, M.P., Michalak, A., and Ziegler, T. (2009). A combined charge and energy decomposition scheme for bond analysis. J. Chem. Theor. Comput. *5*, 962–975.

54. van Lenthe, E., and Baerends, E.J. (2003). Optimized slater-type basis sets for the elements 1-118. J. Comput. Chem. *24*, 1142–1156.

55. te Velde, G., Bickelhaupt, F.M., Baerends, E.J., Fonseca Guerra, C., van Gisbergen, S.J.A., Snijders, J.G., and Ziegler, T. (2001). Chemistry with ADF. J. Comput. Chem. *22*, 931–967.